

localized antisymmetric stretching motion of the CD₂ group. Such a motion must be associated with a nonzero magnetic dipole transition moment. The weakness of the rotatory strength is probably a consequence of the near orthogonality of the electric and magnetic dipole transition moments.

Further discussion of the origin of the VCD intensities in the three chiral species is deferred until additional data become available. We note in passing that all of the stronger VCD bands in the mid-IR region of all species involve coupling to deformations of the three-membered ring. This may be taken to be substantiating evidence for the ring-current mechanism advocated by Nafie and co-workers.⁸

Conclusions

An ab initio implementation of the vibronic coupling theory of Nafie and Freedman²⁹ is described and applied to the computation of VCD intensities of (*S*)-2-deuteriooxirane, (*S,S*)-2,3-dideuteriooxirane, and (*S*)-2,2,3-trideuteriooxirane. The theory is found to reproduce the spectral features of the (*S,S*)-2,3-dideuteriooxirane molecule very well if due consideration is given to the choice of the basis set. The basis set must incorporate derivatives of the normal set of basis functions, a conclusion also reached by others.⁴⁴⁻⁴⁸ Such a basis set, based on the standard 6-31g set and designated 6-31g̃(-2s,2p̄,2p̄_H), is found to yield a geometry for oxirane that is closer to the microwave structure than obtained by optimization with the comparably sized 6-31g** set. Uniform scaling or temperature nonuniform scaling of the 6-31g̃(-2s,2p̄,2p̄_H) force constants permits excellent agreement (<1% error) with observed vibrational frequencies of oxirane and tet-

radeuteriooxirane. Quite satisfactory agreement with the measured IR intensities for these two compounds is also obtained. The effect of nonuniform scaling of the force constants is slightly adverse, suggesting that the ab initio normal modes are somewhat superior to those obtained as a result of adjustments to the force field by the normal procedure.^{5,50,53,54} It is not known whether this observation can be generalized to other molecules or to VCD intensities even of chiral oxiranes.

The APT theory of VCD intensities introduced by Nafie and Freedman²⁸ has been tested against the vibronic coupling theory. Ab initio atomic polar tensors that accurately reproduce the IR spectrum of oxirane and the *d*₄ species were employed. The APT theory was found to have no predictive capability except possibly in the C-D and C-H stretching region of the spectrum. We recommend against its use.

The full IR spectra of all of the deuterated isotopomers of oxirane and the VCD spectra of all of the chiral species are predicted.

Acknowledgment. We express our gratitude to R. A. Shaw for making his "scaling program" available to us. We thank L. A. Nafie and T. B. Freedman for communicating the VCD data of (*S,S*)-2,3-dideuteriooxirane prior to publication and P. J. Stephens for helpful comments on the manuscript. This work was supported by the Natural Sciences and Engineering Research Council of Canada (NSERCC) and in the early stages by a Graduate Scholarship to R.D. from the Killam Foundation. We also thank Supercomputer Services of the University of Calgary for a generous amount of time on the CDC Cyber205 supercomputer.

Synthesis and Characterization of DNA Oligomers and Duplexes Containing Covalently Attached Molecular Labels: Comparison of Biotin, Fluorescein, and Pyrene Labels by Thermodynamic and Optical Spectroscopic Measurements

Joshua Telser,[†] Kenneth A. Cruickshank, Larry E. Morrison, and Thomas L. Netzel*

Contribution from the Amoco Technology Company, Amoco Research Center, P.O. Box 400, Naperville, Illinois 60566. Received June 24, 1988

Abstract: A series of oligonucleotides having the base sequence 5'-GCA(C*-L)(T*-L)CAG-3' have been synthesized where C* and T* are respectively a chemically modified cytidine or thymidine base containing a linker arm terminating in either a primary amine or a molecular label (L) such as biotin, fluorescein, or pyrene. Each oligomer contained a maximum of one chemically modified base. Additionally, the corresponding unmodified oligomers and their complementary unmodified strands were also synthesized. The results of absorption and fluorescence measurements as well as melting temperature studies on these oligomers and their corresponding duplexes are described. Duplexes formed from oligomers containing a T* base exhibited normal melting curve behavior, while those containing a C* base in some cases did not. As a result, thermodynamic parameters for duplex formation were determined only for the former cases. Fluorescence quantum yields were also measured for the T* fluorophore-labeled oligomers both as single strands and as duplexes. Both emission quenching and duplex stabilization indicated strong duplex association (perhaps intercalation) by the covalently attached pyrene labels. No such effects were seen in the duplex formed with the fluorescein-labeled oligomer. The results are discussed in terms of the requirements for achieving good hybridization with labeled oligomers, and in the case of the fluorophore-labeled oligomers, high emission quantum yields from their duplexes.

The base-pairing property of oligomeric strands of DNA allows specific recognition of a particular base sequence in a target strand by a complementary base sequence in a probe strand. However, since DNA probe strands do not naturally contain any convenient

reporter groups, spectroscopic monitoring of hybridization is difficult except in ideally controlled settings. A method to overcome this problem is to prepare a synthetic oligonucleotide with the desired base sequence that also contains a covalently attached molecule label (or reporter group). This label is selected to be easily detectable. For example, direct spectroscopic observation by optical absorption or emission is possible, or as in the case of biotin as a reporter group, enzymatic methods and colorimetric

* To whom correspondence should be addressed.

[†] Present address: Squibb Institute for Medical Research PO Box 191, New Brunswick, NJ 08903.

detection can be used. It may or may not be desirable to separate hybridized and unhybridized probe strands, depending on the physical properties of the probe's label.

A number of workers have developed methods of preparing DNA or RNA oligomers with covalently attached labels. One approach is to modify chemically the heterocyclic base of a nucleoside to provide a functional group amenable to subsequent labeling reactions. Examples of this approach include chemical attachment of aliphatic amines to cytidine at N-4 via a bisulfite-catalyzed transamination reaction^{1,2} and chemical attachment of aliphatic amines to uridine at C-5 via a palladium-mediated olefination reaction.^{3,4} Individual modified nucleosides may be incorporated in DNA strands by using either chemical or enzymatic methods. Dreyer and Dervan⁴ prepared phosphoramidites of labeled uridines and attached them to DNA strands using solid-phase synthesis. Modified nucleoside triphosphates have been enzymatically incorporated at 3'-terminal positions of DNA strands by using terminal deoxynucleotidyl transferase^{5,6} or incorporated within replicated or transcribed DNA or RNA strands by using various polymerases.^{2,3} Attachment of labels to the modified nucleosides has been performed both prior to²⁻⁴ and subsequent to^{5,6} incorporation of the modified nucleosides into polynucleotides.

Another approach to polynucleotide labeling is chemical modification of the phosphate backbone. Labels have been placed at 5'-terminal positions of polynucleotides by condensing the terminal phosphates with ethylenediamine⁷ followed by reaction of the resulting (aminoethyl)phosphoramidates with amine-reactive labeling compounds.⁶ Labels have been placed on internucleotide phosphates during solid-phase synthesis of DNA and include nonchromophoric pendant groups,⁸ a phenanthridium moiety,⁹ and pyrene.¹⁰ The attachment of an acridine derivative to 3'- or 5'-terminal phosphorus has also been reported.¹¹⁻¹⁵

Chemical modification of the bases themselves is the method used in this work. Two types of modifications were used. The first was that developed by Dreyer and Dervan,⁴ who synthesized a derivative of thymidine in which a seven-atom linker arm terminating in a primary amine was attached to the pyrimidine ring at C-5. This is more precisely a uridine derivative, but for consistency with DNA systems it will be referred to here as a thymidine derivative. These workers reacted this modified thymidine with an Fe-EDTA molecule for DNA footprinting studies. The second base modification was related to work by Gillam and Tener,² who used the transamination reaction between cytidine and 1,6-diaminohexane to yield a derivative of cytidine in which

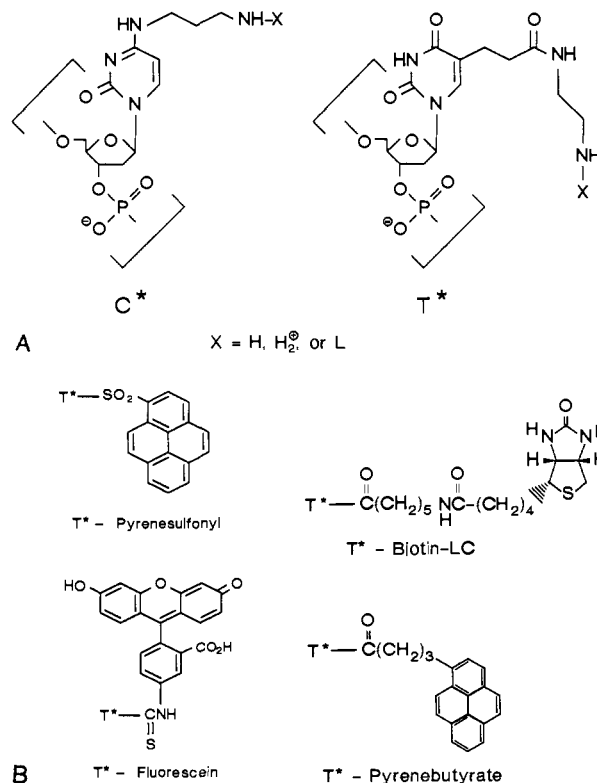


Figure 1. (A) Structures of the modified cytidine (C*) and thymidine (T*) bases as units in an oligonucleotide. The site of label attachment is indicated by X (X = H or H₂⁺ for a modified, unlabeled oligomer and X = L for an attached label). (B) Structures of the molecular labels used in this study in the form in which they are attached to the oligomer. The site of attachment to the oligomer is indicated by T*.

Table I. Duplex Thermodynamic Parameters^a

sequence	ΔH° ($\pm 5\%$), kcal/mol	ΔS° ($\pm 10\%$), cal/(mol K)	ΔG° ($\pm 5\%$), kcal/mol
GCACTCAG	-56 (-58) ^b	-150 (-160) ^b	-10.9 (-10.5) ^b
GCA(C*)TCAG	-56	-160	-9.8
GCAC(T*)CAG	-54 (-58) ^b	-150 (-161) ^b	-9.9 (-9.8) ^b
T*-biotin-LC	-52 (54) ^b	-140 (-150) ^b	-9.2 (-9.2) ^b
T*-fluorescein	-41	-110	-8.9
T*-pyrenebutyrate	-54	-140	-11.4
T*-pyrenesulfonate	-44	-110	-10.0
GCAATCAG	-42	-110	-8.5
GCACCAG	-50	-140	-9.9

^a Parameters at 25 °C. All duplexes were in the T_m buffer = 0.01 M Na₂HPO₄, 0.1 mM Na₂EDTA, 1 M NaCl, pH 7. ^b Values in parentheses are for data taken on a Cary 17 single-sample T_m system.

an eight-atom linker arm was attached to N-4. These workers biotinylated this modified cytidine for enzymatic detection assays.

For convenience, the structural form of the modified thymidine as incorporated into oligonucleotides will be hereafter referred to as T*, and the modified cytidine as C*, with further description as needed. These structures are presented in Figure 1A. In this study, 1,3-diaminopropane was used for the transamination reaction with cytidine rather than 1,6-diaminohexane as done by Gillam and Tener.² The synthesis of these modified nucleotides is presented in Schemes I and II for C* and T*, respectively (see Experimental Section). Figure 1B presents the structures of the molecular labels used in this study. These are shown in the form in which they are attached to DNA via the terminal primary amine of the linker arm of the T* base (C* as identical). An amide linkage to DNA is formed with sulfosuccinimidyl 6-(biotinamido)hexanoate. Fluorescein-5-isothiocyanate reacts with the primary amine to give a thiourea linkage. Succinimidyl 1-pyre-

(1) Draper, D. E. *Nucleic Acids Res.* **1984**, *12*, 989.

(2) Gillam, I. C.; Tener, G. M. *Anal. Biochem.* **1986**, *157*, 199.

(3) Langer, P. R.; Waldrop, A. A.; Ward, D. C. *Proc. Natl. Acad. Sci. U.S.A.* **1981**, *78*, 6633.

(4) Dreyer, G. B.; Dervan, P. B. *Proc. Natl. Acad. Sci. U.S.A.* **1985**, *82*, 968.

(5) Eshaghpour, H.; Soll, D.; Crothers, D. M. *Nucleic Acids Res.* **1979**, *7*, 1485.

(6) Morrison, L. E. European Patent Application, 1987, publication number 0232967.

(7) Chu, B. C. F.; Wahl, G. M.; Orgel, L. E. *Nucleic Acids Res.* **1983**, *11*, 6513.

(8) Letsinger, R. L.; Bach, S. A.; Eadie, J. S. *Nucleic Acids Res.* **1986**, *14*, 3487.

(9) Letsinger, R. L.; Schott, M. E. *J. Am. Chem. Soc.* **1981**, *103*, 7394.

(10) Yamana, K.; Letsinger, R. L. *Nucleic Acids Symp. Ser.* **1985**, *16*, 169.

(11) Asseline, U.; Thuong, N. T.; Helene, C. *C. R. Acad. Sci. Paris* **1983**, *297 (III)*, 369.

(12) Asseline, U.; Delarue, M.; Lancelot, G.; Toulme, F.; Thuong, N. T.; Montenay-Garestier, T.; Helene, C. *Proc. Natl. Acad. Sci. U.S.A.* **1984**, *81*, 3297.

(13) Asseline, U.; Toulme, F.; Thuong, N. T.; Delarue, M.; Montenay-Garestier, T.; Helene, C. *EMBO J.* **1984**, *3*, 795.

(14) Asseline, U.; Thuong, N. T.; Helene, C. *Nucleosides Nucleotides* **1986**, *5*, 45.

(15) Helene, C.; Toulme, F.; Delarue, M.; Asseline, U.; Takasugi, M.; Maurizot, M.; Montenay-Garestier, T.; Thuong, N. T. In *Biomolecular Stereodynamics III*; Sarma, R. H., Sarma, M. H., Eds.; Adenine Press: New York, 1986; pp 119-130.

nebutyrate and 1-pyrenesulfonyl chloride react to give respectively amide and sulfonamide linkages to DNA. These pendant molecular labels will, for simplicity, be referred to hereafter as follows: biotin, fluorescein, pyrenebutyrate, and pyrenesulfonate.

We have prepared a series of octamers, which are listed in Table I, all with the sequence 5'-GCACTCAG-3' or its complement, 5'-CTGAGTGC-3'. The oligomers differ in that they contain either a modified thymidine or cytidine to give the following actual sequences: 5'-GCAC(T*-L)CAG-3' or 5'-GCA(C*-L)TCAG-3', where L = a label such as biotin, fluorescein, pyrenebutyrate, or pyrenesulfonate.

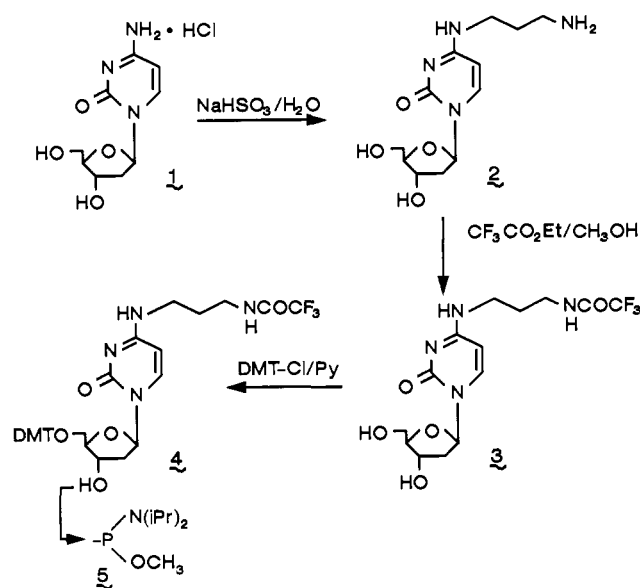
There were several objectives to this work. The first was to determine whether or not oligomers containing the primary amine-functionalized bases could be synthesized by using standard automated procedures such that these modified oligomers would react efficiently and specifically with various molecular labels to give isolable, labeled oligomers. Ideally, an arbitrary sequence could then be selected that would contain a modified base in an arbitrary but strategic location. The resulting modified oligomer could then be labeled with one of a number of molecular labels. While much previous work has consisted of label attachment at the 3'- or 5'-termini of an oligonucleotide,^{6,15,17} it is also important to show that internal labeling is a viable synthetic route, since this could give greater flexibility in the design of labeled oligomers. Given the ability to synthesize these internally labeled oligonucleotides, it is then necessary to confirm that covalent attachment of the label does not adversely affect either the labels themselves or the modified oligonucleotides. The first effect can be determined by measuring the optical spectra and relative emission quantum yields of the fluorophore-labeled oligomers, both as single strands and as duplexes. The second effect can be determined by making melting temperature (T_m) measurements as a function of DNA concentration for the series of oligomers and their complementary strands. This allows calculation of thermodynamic parameters for duplex formation.

Experimental Section

General. All chemicals were used as obtained unless otherwise stated. Thin-layer chromatography (TLC) was performed on glass-backed plates of Merck 60F-254 silica gel. All 4,4'-dimethoxytrityl-containing substances were identified as orange colored spots on TLC plates by spraying with a fine mist of concentrated sulfuric acid-ethanol (1:1, v/v). Active phosphoramidites were hydrolyzed by acetonitrile-water (95:5, v/v) containing 0.1 M tetrazole to ascertain purity. Fast-atom bombardment mass spectra were recorded on a VG 70 250SE mass spectrometer. Proton NMR spectra were recorded at 300 MHz on a Varian EXR 300 nuclear magnetic resonance spectrometer unless otherwise stated. Qualitative UV-visible spectra were recorded on a Hewlett-Packard 8451A diode array spectrophotometer.

Synthetic Procedure for Substances Illustrated in Scheme I. *N*⁴-(3-Aminopropyl)-2'-deoxycytidine (2, Scheme I). A solution of sodium metabisulfite (8.8 g, 46.3 mmol), 1,3-diaminopropane (3.0 g, 40.5 mmol), and 2'-deoxycytidine hydrochloride (1, 2.0 g, 7.6 mmol) in deionized water (40 mL) was adjusted to pH 7.1 by addition of 1,3-diaminopropane or metabisulfite. The resulting solution was tightly capped and incubated at 37 °C for 7 days or until analysis by TLC using concentrated ammonia-isopropyl alcohol-water (35/55/10, v/v) revealed that more than 95% of the substrate had reacted to give a lower R_f , ninhydrin-positive substance. The reaction mixture was added to freshly prepared Dowex 50X-200 ion exchange resin (H⁺ form, 200 mL), which had been taken through three ion exchange/regeneration cycles using 1 M NaOH, deionized water, 1 M HCl, and deionized water. The mixture was left in a hood overnight (Caution: fumes of SO₂ are evolved!). The mixture was poured onto a bed of fresh resin (10 mL) in a glass column (final bed dimension 70 cm × 2.6 cm diameter; attached to a Gilson HM Holochrome UV monitor and Gilson FC-80K fractionator) and eluted with water until the UV absorbance of the eluant had stabilized. The column was then eluted with a linear gradient (1 L) of 0–5% ammonium hydroxide in methanol-water (1:1, v/v). When the product began to elute, the ammonium hydroxide concentration was increased to 15% (v/v) and maintained at this concentration until elution of the product

Scheme I



was complete. Fractions containing the product were evaporated, then coevaporated with ethanol (3 × 80 mL), and finally dried under vacuum to a thick oil; yield 2.0 g, 7.2 mmol, 97.3%.

*N*⁴-(3-(*N*-(Trifluoroacetyl)amino)propyl)-2'-deoxycytidine (2, Scheme I). The crude preparation of *N*⁴-(3-aminopropyl)-2'-deoxycytidine (2, 2 g, 7.2 mmol) was dissolved in methanol (50 mL), and ethyl trifluoroacetate (3.1 mL, 26 mmol) was added. The reaction mixture was stirred for 24 h under anhydrous conditions at which time TLC using chloroform-methanol (4:1, v/v) showed the reaction was complete. The solution was evaporated to dryness and coevaporated with ethanol (2 × 50 mL) to give a thick oil (2.91 g). The substance was dissolved in a minimum volume of ethyl acetate-methanol (1:1, v/v); silica gel (25 mL) was added, and the mixture evaporated to dryness in vacuo. The resulting powder was applied to a short column (300 mL) of dry silica gel. A stepped gradient of 5, 10, 15, and 20% ethyl acetate in methanol (v/v, 800 mL each) was used to elute the column. The product-containing fractions were combined and evaporated; yield 1.20 g, 3.2 mmol, 44%. ¹H NMR (200 MHz, DMSO-*d*₆) 9.47 (br s, ex, 1 H, NH), 7.74 (m, 2 H, H-6 and NH), 6.16 (t, $J = 6.4$ Hz, 1 H, H-1'), 5.74 (d, $J = 7.5$ Hz, 1 H, H-5), 5.19 (d, ex, $J = 4.2$ Hz, 3'-OH), 4.97 (t, ex, $J = 5.3$ Hz, 5'-OH), 4.19 (m, 1 H, H-3'), 3.76 (m, 1 H, H-4'), 3.54 (m, 2 H, H-5' and H-5''), 3.24 (q, $J = 6.7$ Hz, 4 H, 2 × NCH₂), 2.08 (m, 1 H, H-2'), 1.94 (m, 1 H, H-2''), 1.71 (q, $J = 7.0$ Hz, 2 H, CH₂). UV (methanol) λ_{max} 274 nm.

*N*⁴-(3-(*N*-(Trifluoroacetyl)amino)propyl)-5'-dimethoxytrityl-2'-deoxycytidine (4, Scheme I). To a solution of compound 3 (1.22 g, 3.21 mmol) in anhydrous pyridine (10 mL) containing 4-(dimethylamino)pyridine (0.020 g, 0.160 mmol) and triethylamine (0.454 g, 4.49 mmol) was added 4,4'-dimethoxytrityl chloride (1.305 g, 3.85 mmol). The resulting mixture was magnetically stirred at room temperature for 2 h, when TLC (chloroform-methanol, 4:1, v/v) revealed that the reaction was complete to give a higher R_f substance. The solvent was evaporated in vacuo; the residue was dissolved in chloroform (100 mL) and extracted with saturated sodium hydrogen carbonate solution (100 mL). The organic layer was dried (NaSO₄) and evaporated to give an orange gum which was further purified by flash chromatography on silica gel. Elution with increasing amounts of methanol in ethyl acetate (0–5%, v/v) containing triethylamine (2%, v/v) eluted the product; yield 1.816 g, 2.54 mmol, 79%.

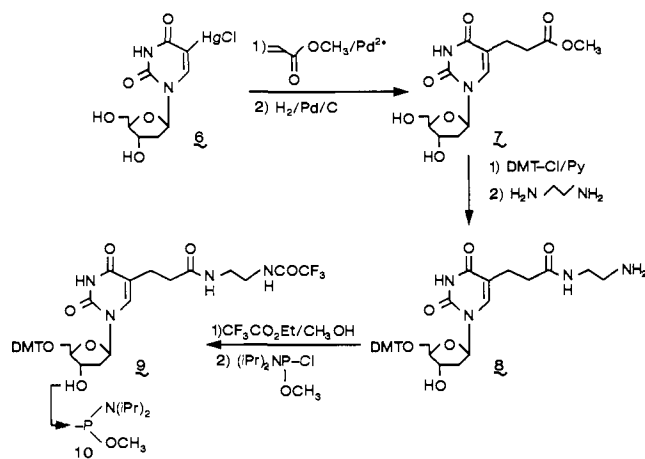
*N*⁴-(3-(*N*-(Trifluoroacetyl)amino)propyl)-5'-dimethoxytrityl-2'-deoxycytidine-3'-(*O*-methyl-*N,N*-disopropyl)phosphoramidate (5, Scheme I). This was prepared from compound 4 (1.816 g, 2.54 mmol) by using the same methods as described below for compound 10 (see Scheme II); yield 2.31 g, 2.18 mmol, 82%. The colorless foam obtained from flash chromatography on silica gel was coevaporated with anhydrous acetonitrile (6 × 40 mL), immediately prior to preparation of a 0.1 M acetonitrile solution required for phosphoramidite synthesis.

Synthetic Procedure for Substances Illustrated in Scheme II. 2'-Deoxyuridine-5-(propionic acid methyl ester) (7, Scheme II). 5-Chloromercuro-2'-deoxyuridine (6) was prepared and reacted with methyl acrylate under the conditions described by Dreyer and Dervan.⁴ 2'-Deoxyuridine-5-(propenoic acid methyl ester) (3.4 g, 10.9 mmol) was dissolved in methanol (200 mL), and charcoal (0.77 g) was added. The

(16) Caruthers, M. *Science* **1985**, *230*, 281.

(17) Heller, M. J.; Morrison, L. E. In *Rapid Identification and Detection of Infectious Agents*; Kingsbury, D. T., Falkow, S., Eds.; Academic Press: New York, 1985; pp 245–256.

Scheme II



mixture was stirred for 10 min, and the solution filtered and diluted to a total volume of 350 mL with methanol. This procedure enabled the subsequent catalytic hydrogenation to proceed smoothly, because catalyst poisons were removed by the charcoal. To the methanol solution of the nucleoside was added hydrogenation catalyst (10% Pd/C, 0.51 g, Alfa), and the mixture was hydrogenated with stirring in a Parr reactor (65 psi H₂, 22 h), TLC (ethyl acetate–methanol, 85:15 v/v) showed that the reduction was complete. The reaction mixture was then filtered through a 0.22- μ m Acrodisc filter to remove all catalyst and evaporated to dryness; yield 2.9 g, 8.94 mmol, 82%. UV (methanol) λ_{max} 212, 268 nm.

5'-Dimethoxytrityl-2'-deoxyuridine-5-[N-(2-aminoethyl)propionamide (8, Scheme II). Compound 7 was converted to the 5'-dimethoxytrityl derivative by methods described previously (see Scheme I).⁴ ¹H NMR (CDCl₃) 7.52 (s, 1 H, H-6), 7.40 (m, 2 H, DMT), 7.33–7.20 (m, 7 H, DMT), 6.83 (m, 4 H, DMT), 6.36 (t, *J* = 6.3 Hz, H-1'), 4.55 (m, 1 H, H-3'), 4.04 (m, 1 H, H-4'), 3.72 (s, 6 H, 2 × OCH₃), 3.59 (s, 3 H, CO₂CH₃), 3.42 (m, 2 H, H-5', H-5''), 2.43–2.20 (m, 6 H, H-2', H-2'', 2 × CH₂). High-resolution FAB mass spectrum: obsd 617.237; calcd for C₃₄H₃₇N₂O₈, 617.250. This compound was then converted to the ethylenediamine adduct (8) by ester–amide exchange with ethylenediamine as described by Dreyer and Dervan. The physical properties and spectroscopic data were identical with those reported.⁴

5'-Dimethoxytrityl-2'-deoxyuridine-5-[2-(N-(trifluoroacetyl)amino)ethyl]propionamide (9, Scheme II). Compound 8 (0.999 g, 1.62 mmol) was dissolved in methanol (10 mL) containing triethylamine (0.5 mL), and ethyl trifluoroacetate (1.381 g, 9.72 mmol) was added. The resulting mixture was stirred at room temperature for 16 h when TLC (chloroform–methanol, 4:1, v/v) indicated complete conversion to a higher *R_f* substance. The mixture was evaporated to dryness, and the residue purified by flash chromatography on silica gel. Gradient elution with increasing quantities of methanol in ethyl acetate (0–4%, v/v) containing triethylamine (2%, v/v) eluted compound 9; yield 0.88 g, 1.23 mmol, 76%. ¹H NMR (CDCl₃) 8.08 (br s, 1 H, NH), 7.60 (s, 1 H, H-6), 7.42–7.29 (m, 9 H, DMT), 6.85 (m, 4 H, DMT), 6.35 (t, *J* = 6.2 Hz, 1 H, H-1'), 6.23 (t, *J* = 6 Hz, 1 H, OH), 4.54 (m, 1 H, H-3'), 4.05 (m, 1 H, H-4'), 3.79 (s, 6 H, 2 × OCH₃), 3.48 (m, 1 H, H-5'), 3.39–3.24 (m, 5 H, 2 × NCH₂, H-5''), 2.60 (q, *J* = 5 Hz, 2 H, CH₂), 2.26 (m, 2 H, H-2', H-2''), 2.12 (m, 2 H, CH₂). Positive ion FAB MS: 763 (MNa⁺, 60%), 675 (15), 631 (14), 569 (16), 525 (14), 481 (23), 393 (42), 345 (68), 303 (100). High-resolution FAB MS: obsd 763.257; calcd for C₃₇H₃₉N₄O₉F₃Na, 763.257.

5'-Dimethoxytrityl-2'-deoxyuridine-5-[2-(N-(trifluoroacetyl)amino)ethyl]propionamide-3'-(*O*-methyl(diisopropylamino))phosphoramidate (10, Scheme II). Compound 9 (0.520 g, 0.728 mmol) was dissolved in anhydrous dichloromethane (2.5 mL) containing diisopropylethylamine (0.42 mL, 2.422 mmol), and *N,N*-diisopropylmethylphosphonamidic chloride (0.215 g, 1.5 mmol) was added by syringe to the magnetically stirred solution. After 1 h, TLC (on prerun plates; methanol–chloroform–triethylamine, 10/85/5, v/v/v) indicated that the reaction was complete. The reaction mixture was added to ethyl acetate (75 mL) that had been prewashed with saturated sodium hydrogen carbonate and was extracted with saturated sodium hydrogen carbonate solution (75 mL). The organic layer was dried over anhydrous sodium sulfate and evaporated to a pale-yellow oil which was further purified by flash chromatography on silica gel. Elution with ethyl acetate–triethylamine (98:2, v/v) yielded the active amidite (10) as a TLC homogeneous, colorless foam; yield: 0.54 g, 0.62 mmol, 85%. The product was coevaporated six times with anhydrous acetonitrile and finally dissolved in acetonitrile to

give a 0.1 M solution used in automated oligonucleotide synthesis.

Oligonucleotide Synthesis. Oligonucleotides containing either modified or unmodified bases were synthesized on an Applied Biosystems Model 380B DNA synthesizer using, unless otherwise stated, protocols and reagents obtained from Applied Biosystems. Acetonitrile used by the automated DNA synthesizer was distilled from powdered calcium hydride immediately before use.

Oligonucleotide Purification. The crude reaction product from the automated oligonucleotide synthesis was purified by using a Pharmacia FPLC system equipped with a ProRPC HR 10/10 column (100 mm × 10 mm diameter, packed with a silica-based 13- μ m C2/C8 matrix of 300-Å pore size). First a linear gradient of 1:1 (v/v) acetonitrile/10 mM triethylammonium acetate against 10 mM triethylammonium acetate was used ranging from 0 to 35% over 45 min at 2 mL/min. This separation was followed by a second run using the same solvent system with a gradient ranging from 0 to 70% at the same rate. This latter protocol was also used to purify the labeled oligomers. The fractions were monitored by absorption at 254 nm.

Synthesis of Labeled Oligonucleotides. A lyophilized sample of a chemically modified oligomer (containing C* or T*, approximately 5 optical density (OD)) was dissolved in sodium borate buffer (pH = 9.3, 0.75 mL) in a disposable 2-mL sample vial. To this was added a solution of the desired label in *N,N*-dimethylformamide (DMF, approximately 150-fold excess, 0.25 mL). In the case of the pyrene derivatives, this was a DMF suspension. The reaction mixture was stirred vigorously at room temperature for approximately 12 h in the dark, centrifuged, and then run through a Pharmacia Sephadex NAP-10 column to desalt and remove excess label. The resulting solution was purified by using the FPLC system as described above. Due to the small scale of the labeling reaction and losses in material transfer, overall yields varied significantly. Average yields based on recovered labeled oligomer as a fraction of starting modified oligomer are as follows (all \pm 10% and based on several independent reaction runs): biotin, 70%; fluorescein, 70%; pyrenebutyrate, 60%; pyrenesulfonate, 40%. The low water solubility of 1-pyrenesulfonyl chloride causes the lower yield. The following species were used for the labeling reactions (all from Molecular Probes, Eugene, OR; catalog number given): succinimidyl 1-pyrenebutyrate (S-130), 1-pyrenesulfonyl chloride (P-24), and fluorescein-5-isothiocyanate (F-1906, in sealed ampules). For the biotinylation reaction, sulfosuccinimidyl 6-(biotin-amido)hexanoate (NHS-LC-Biotin, Pierce Chemical, Rockford, IL) was used. The following molecules were used for comparison spectra (Molecular Probes): 1-pyrenebutanoic acid (P-32), sodium 1-pyrenesulfonate (P-80), *N*-(1-pyrenesulfonyl)ethylenediamine (P-168), and 5-((2-aminoethyl)thioureidyl)fluorescein (A-458).

Enzymatic Degradation. Modified and unmodified oligomers were converted to their constituent nucleosides by sequential reaction with phosphodiesterase I and alkaline phosphatase. An oligomer (0.7 OD) was allowed to react for 1 h at 37 °C with phosphodiesterase I (5 units, Pharmacia LKB Biotechnology, Piscataway, NJ) in 100 μ L of buffer (0.1 M NaCl, 14 mM MgCl₂, and 0.1 M Tris, pH = 8.9). To this was added calf intestinal alkaline phosphatase (30 units, Promega Biotec, Madison, WI) in 7 μ L of buffer (10 mM MgCl₂, 1 mM ZnCl₂, and 0.5 M Tris, pH = 9.0) and the reaction allowed further to proceed for 1 h at 37 °C. An aliquot of the reaction (20–50 μ L) was then analyzed on a Pharmacia FPLC system equipped with a MinRPC column. A linear gradient of 20% (v/v) methanol/50 mM KH₂PO₄ (pH = 4.0) versus 2.5% (v/v) methanol/50 mM KH₂PO₄ (pH = 4.0) was used ranging from 0 to 100% over 50 min at 0.4 mL/min. This was followed by further elution with the 20% methanol buffer for 10 min.

Spectroscopic Measurements. UV–visible absorption spectra were recorded on a Perkin-Elmer Lambda 9 UV/vis/NIR spectrophotometer. Fluorescence emission and excitation spectra were recorded on a SLM/Aminco SPF-500C fluorometer controlled by an IBM-PC/AT using SLM software. Fluorescence quantum yield measurements were made by using a polarizer in the excitation beam set at 35.3° with respect to the vertical direction and an achromatic wedge depolarizer between the sample cell and the detection monochromator. This setup corrects for rotational depolarization effects.¹⁹ The spectra were corrected for both buffer background and the wavelength-dependent response of the fluorometer. Emission quantum yields for the pyrenebutyrate and pyrenesulfonate-labeled oligomers are reported relative to the emission of pyrenebutyrate or pyrenesulfonate, respectively, in aerated *T_m* buffer solutions (see below). Absolute quantum yields of pyrenebutyrate and pyrenesulfonate in the *T_m* buffer were determined to be 0.6 and 0.8, respectively, by using quinine sulfate in 0.1 M H₂SO₄ as a quantum yield standard (quantum yield of quinine sulfate = 0.70 \pm 0.02).²⁰ Quantum

(18) *Oligonucleotide Synthesis: A Practical Approach*, Gait, M. J., Ed.; IRL Press: Oxford, UK, 1984; pp 35–81.

(19) Spencer, R. D.; Weber, G. *J. Chem. Phys.* 1970, 52, 1654.

yields of the fluorescein-labeled oligomers are reported relative to fluorescein in 0.1 M NaOH (absolute quantum yield of 0.92).²¹ The relative quantum yields within an isolabeled series are accurate to $\pm 10\%$.

Measurement of Melting Curves. Two melting curve measurement systems were used: a single-sample system based on a Cary 17 UV/vis spectrophotometer and a multisample system to be described below. T_m measurements were made using both systems on the unmodified duplex, the T*-containing unlabeled duplex, and the T* duplex labeled with biotin. All other T_m determinations were made only on the multisample system which was fully automated and controlled by an IBM-PC/AT. In this case the computer controlled a Perkin-Elmer Lambda 9 spectrophotometer through an RS-232 communication port, a Neslab Endocal refrigerated circulating bath via a Data Translation 2805 D/A board, and a Keithley 705 scanner box connected to a 193A digital multimeter via a National Instruments GPIB-PC board. The Lambda 9 was equipped with a programmable six-cell holder. This allowed measurement of up to five samples during a single run; one cell was reserved for a blank solution to allow zeroing of the spectrophotometer during the run. The temperature of each sample was measured simultaneously with its absorbance. The samples were held in quartz 1-cm path length microcuvettes (sample volume 1.4 mL). Each cuvette was sealed by a Teflon stopper through which a stainless steel encapsulated thermistor was press-fitted. The thermistors were custom made by Thermometrics (Edison, NJ) and were calibrated over the 0–100 °C range with NBS standards. The melting curves were obtained by slowly heating the samples to the high end of the run (60–80 °C) and allowing equilibration for 20 min. The samples were then cooled to the low end of the run (0–10 °C) at a rate of 10 °C/h. The bath temperature was decremented in 1 °C steps, and approximately 30 absorbance readings at 260 nm were made and averaged at each temperature. The samples were then heated at this same rate back to the high temperature. Very little hysteresis was observed. At the end the samples were rapidly cooled to room temperature. The recorded temperatures are accurate to ± 0.1 °C, and the absorbance values are accurate to ± 0.002 OD. The main error in the resulting thermodynamic determinations arises from inaccuracies in DNA concentration. Literature values were used to determine extinction coefficients for the unmodified octamers.²² To account for label absorbance at 260 nm in the labeled oligomers, the absorption of the free label at 260 nm was compared to that of one of its bands beyond 300 nm, where DNA has no absorption. The absorption of the labeled oligomer at 260 nm would then be corrected for label absorption by using the above ratio of free label absorbance at 260 nm to that beyond 300 nm and the measured absorbance in the labeled oligomer beyond 300 nm. The DNA concentration would be determined from this corrected absorbance and the extinction coefficient for the corresponding unmodified oligomer. This procedure makes the assumption that the extinction coefficient of the label when attached to single-strand DNA is the same as that for the free label. This assumption is inherently inaccurate but is reasonable since the absorption spectra of variously labeled single-strand DNA showed virtually no temperature dependence, suggesting that attachment to DNA has little effect on the label's absorption properties. The procedure for a series of concentrations was to make a stock solution of a duplex (absorbance of 3) and then run melting curves of this solution diluted by factors of 2 until the helix-to-coil transition was barely observable (duplex absorbance approximately 0.1 OD). With the multicell system, it was possible to record T_m curves for up to five samples during one run. The buffer system used for the T_m determinations was 10 mM dibasic sodium phosphate, 0.1 mM sodium EDTA, and 1 M NaCl (Aesar, Puratronic grade), adjusted to pH 7 by using NaOH.

Analysis of Melting Curves. The melting curves obtained in the above manner were fitted by using the nonlinear least-squares program DSTSEPT, obtained from the Quantum Chemistry Program Exchange, Bloomington, IN (program no. 307). The program was modified to include a subroutine to calculate theoretical values using the "all-or-none" model of DNA hybridization originally described by Applequist and Damle.²³ This provided an accurate method of determining the T_m of each sample within a concentration series. The fitting procedure yielded values of ΔH° and ΔS° for an individual melting curve. While these values were consistent with those determined by using the method described below, they had significantly more error and were therefore of little quantitative use. The reported thermodynamic parameters were derived from a graph of $1/T_m$ versus \ln (DNA concentration), which was fitted to a linear least-squares equation to give ΔH° and ΔS° . This procedure is described

in detail by Marky and Breslauer.²⁴

Error Analysis of Melting Curves. Since two different T_m determination systems, each using independently prepared oligonucleotides, were used to study three duplexes, comparison of these results provides a good estimate of the total error in the thermodynamic parameters measured for duplex formation. Estimating the overall error resulting from inaccuracies in our knowledge of temperature, absorbance, concentration, etc., is difficult and most likely less informative than this overall comparison. Table I presents the values for ΔH° , ΔS° , and ΔG° for the dual determinations on three duplexes. The variations suggest that the values of ΔH° and ΔG° are reproducible to within 5% and ΔS° to within 10%. Similar errors are estimated by Freier et al.²⁵ ΔS° is inherently less well determined than ΔH° since it is obtained from the y intercept and slope rather than just the slope in the graph of $1/T_m$ versus \ln (DNA concentration).

Results and Discussion

The specific base sequence for the octamer used in this study, 5'-GCACTCAG-3', was selected for several reasons. First, an octameric length produced a stable duplex, with a convenient T_m . Additionally, guanosine/cytidine pairs were positioned at the duplex ends to prevent fraying,²⁶ while thymidine and cytidine bases were positioned near the center to allow labeling. All four types of heterocyclic bases were used in both the labeled strand and its complement, so that the generality of the labeling reactions could be tested. Finally, this sequence resembled others that had been previously studied and found to have the normal B-DNA structure.²⁷

The labels used in this study were also selected for reasons of generality. Biotin is useful for enzyme-based colorimetric label-detection assays, while fluorescein and the two pyrenes have good fluorescence properties. Fluorescein is a representative nonassociating organic fluorophore. However, polycyclic aromatic hydrocarbons in general^{28,29} and pyrene in particular^{30,31} are known to associate with natural DNA duplexes under certain conditions. For generality, it was desirable that the modified oligonucleotides be prepared by using automated synthesizer protocols with a minimum of changes relative to the synthesis of unmodified oligonucleotides. Therefore, rather than synthesizing a modified phosphoramidite that already contains an attached label, it is often preferable to synthesize a modified oligonucleotide with a primary amine group available for subsequent labeling. Incorporation of a modified base into an oligonucleotide was confirmed for the oligomer containing the modified thymidine (5'-GCAC(T*)-CAG-3'). This was accomplished by enzymatically digesting the modified oligomer and fractionating the resulting nucleosides by reversed-phase liquid chromatography. The same procedure was performed on the unmodified, parent oligomer. Fractionation of the digested parent oligomer produced four peaks corresponding to the four nucleosides. Fractionation of the digested modified oligomer showed the absence of the peak corresponding to thymidine but exhibited a new peak with greater hydrophobicity. This behavior is expected for the modified thymidine since it contains the relatively hydrophobic linker arm.

The above strategy allows considerable flexibility in the choice of labels and labeling reactions. However, these labeling reactions should be run at pH ≈ 9 to ensure that the primary amine is deprotonated and can thus act as a nucleophile toward the activated label. The aqueous borate buffer used in these reactions is ideal for high pH and good DNA solubility, but many labels

(20) Scott, T. G.; Spencer, R. D.; Leonard, N. J.; Weber, G. *J. Am. Chem. Soc.* **1970**, *92*, 687.

(21) Weber, G.; Teale, F. W. J. *Trans. Faraday Soc.* **1957**, *53*, 646.

(22) *Handbook of Biochemistry and Molecular Biology: Nucleic Acids*, 3rd ed.; CRC Press: Cleveland, OH, 1975; Vol I, p 589.

(23) Applequist, J.; Damle, V. *J. Am. Chem. Soc.* **1965**, *87*, 1450.

(24) Marky, L. A.; Breslauer, K. J. *Biopolymers* **1987**, *26*, 1601.

(25) Freier, S. M.; Alkema, D.; Sinclair, A.; Neilson, T.; Turner, D. H. *Biochemistry* **1985**, *24*, 4533.

(26) Marky, L. A.; Canuel, L.; Jones, R. A.; Breslauer, K. J. *Biophys. Chem.* **1981**, *13*, 141.

(27) Dickerson, R. E.; Drew, H. R.; Conner, B. N.; Wing, R. M.; Fratini, A. V.; Kopka, M. L. *Science* **1982**, *216*, 475.

(28) Hiedelberger, C. *Annu. Rev. Biochem.* **1975**, *44*, 79.

(29) LeBreton, P. R. In *Polycyclic Aromatic Hydrocarbons and Carcinogenesis* Harvey, R. G., Ed.; American Chemical Society: Washington, D.C., 1985; pp 209–238.

(30) Geacintov, N. E.; Prusik, T.; Khosrofiyan, J. M. *J. Am. Chem. Soc.* **1976**, *98*, 6444.

(31) Wolfe, A.; Shimer, G. H., Jr.; Meehan, T. *Biochemistry* **1987**, *26*, 6392.

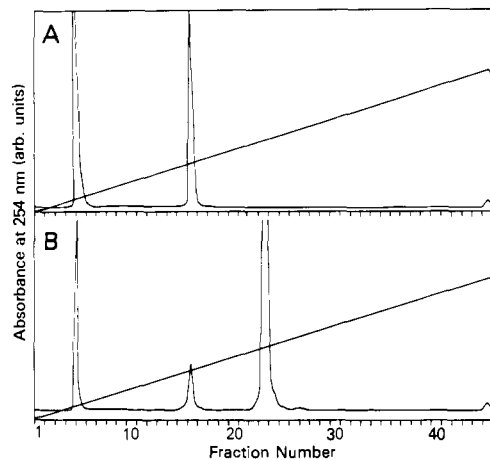


Figure 2. Chromatograms of the reaction between succinimidyl 1-pyrenebutyrate and (A) 5'-GCACTCAG-3' and (B) 5'-GCAC(T*)CAG-3'. The peaks in both chromatograms at fraction 4 and fraction 17 correspond to *N*-hydroxysuccinimide and unreacted DNA, respectively. The peak at fraction 24 in chromatogram B corresponds to the pyrenebutyrate-labeled octanucleotide. The minor peak at fraction 50 corresponds to pyrenebutyrate. Chromatography was carried out with a linear gradient of 1:1 acetonitrile/10 mM triethylammonium acetate against 10 mM triethylammonium acetate ranging from 0 to 70% over 45 min at 2 mL/min with 2-mL fractions on a Pharmacia ProRPC 10/10 column.

(including the ones studied here) are not very soluble in it. This does, however, facilitate their separation from the reaction mixture, and since labels are relatively inexpensive compared to the oligonucleotide, they can be used in large excess. An important concern is that the activated label (containing, for example, an *N*-hydroxysuccinimide ester, a sulfonyl chloride, or an isothiocyanate group) not react with any functional groups on the oligonucleotide other than the intended primary amine.

This study verified that only oligomers containing a modified thymidine or cytidine base with an attached primary amine (C* and T*) gave a reaction product. This result is illustrated in Figure 2, which shows the FPLC traces for the reaction of both the unmodified octamer (2A) and the corresponding T*-modified octamer (2B) with succinimidyl 1-pyrenebutyrate. The absorption spectra (not shown) indicate that fraction 17 in both chromatograms is unreacted DNA, while fraction 24 in chromatogram 2B exhibits absorption bands due to both pyrene and DNA and is thus the pyrene-labeled octamer. In the case of pyrenesulfonate labeling, the appropriate fraction shows formation of the expected sulfonamide linkage (see below). In addition, comparison of these FPLC traces with those of the DNA starting material alone (not shown) indicates that no decomposition of the original DNA octamer occurred. Similar results with both C*- and T*-modified oligomers were obtained for all the other label discussed here. Since it is possible to recover unreacted modified oligomer, the relatively low yields of these labeling reactions are still acceptable (see Experimental Section for overall yields; the FPLC trace is not meant to imply a yield value since it does not take into account material transfer losses). This recycling of valuable starting material is particularly helpful when labeling with the very insoluble 1-pyrenesulfonyl chloride. There is a significant change in the solubility of a DNA octamer as a result of the covalent attachment of a large hydrophobic molecule like pyrene. This fact allows convenient purification of the reaction product using reversed-phase liquid chromatography.

The chemical inertness of the unmodified oligomer toward labeling shows that even for oligomeric sequences containing bases with primary amines (adenosine, guanosine, and cytidine), the above-described labeling strategy is sound. This is probably true for two reasons. First, an aliphatic primary amine is a better nucleophile than are the aryl amines on the heterocyclic bases of DNA; the latter have imino tautomers. Second, the linker arm makes the primary amine more accessible than the amino groups on the heterocyclic bases. Even for a single strand, the latter are

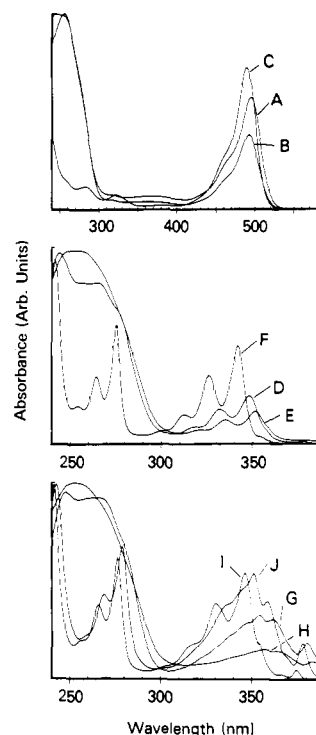


Figure 3. UV-visible absorption spectra of fluorophore-labeled DNA and free fluorophores: (A) fluorescein-labeled single strand; (B) fluorescein-labeled duplex; (C) fluorescein; (D) pyrenebutyrate-labeled single strand; (E) pyrenebutyrate-labeled duplex; (F) pyrenebutyrate; (G) pyrenesulfonate-labeled single strand; (H) pyrenesulfonate-labeled duplex; (I) pyrenesulfonate; (J) *N*-(1-pyrenesulfonyl)ethylenediamine. All samples are in the pH 7 T_m buffer described in the text. The samples have widely varying absorbances, so the spectra have been normalized to allow presentation on the same vertical scale.

probably partially self-associated and thus less available for reaction with the activated label. This specificity of reaction between the modified oligomers and the activated labels is crucial.

It would be desirable to complement this combination of enzymatic, chromatographic, and optical spectroscopic evidence with other techniques to confirm the product identity. NMR spectroscopy has been recently used to determine the solution structure of oligonucleotides.³² However, these studies require concentrated solutions (millimolar) that are difficult to achieve for labeled oligomers. Furthermore, analysis of non-self-complementary duplexes is more complex than for the more commonly studied self-complementary systems, and a labeled system would further complicate matters. Nevertheless, NMR is potentially applicable to these systems.

Spectroscopic Characterization. Given that it is possible to synthesize specifically labeled oligonucleotides, these oligomers and their corresponding duplexes can then be characterized by absorption and emission spectroscopies and by melting temperature determinations. Oligomers labeled at both cytidine (C*) and thymidine (T*) had qualitatively the same optical spectra but differed greatly in melting curve behavior. As will be discussed below, only the oligomers labeled at thymidine gave melting curves that always qualitatively resembled those of the corresponding unlabeled octamers. Therefore, quantitative spectroscopic and thermodynamic data will be presented here only for T* duplexes.

Figure 3 shows that the absorption spectra of the fluorophore-labeled oligomers and their duplexes exhibit the characteristic band of both DNA and the label. For comparison purposes the absorption spectra of the labeled single strands, labeled duplexes, and labels alone are all presented. The label models are fluorescein, *N*-(1-pyrenesulfonyl)ethylenediamine, 1-pyrenebutanoic acid, and sodium 1-pyrenesulfonate. Note that the latter

(32) Gronenborn, A. M.; Clore, G. M. *Prog. NMR Spectrosc.* **1985**, *17*, 1.

Table II. Spectroscopic Data^a

sample	rel quantum yield ($\pm 10\%$)	λ_{\max} , nm	
		abs	emission
fluorescein	1.0 ^b	491	514
5-((2-aminomethyl)thioureidyl)-fluorescein	0.96 ^b	494	516
above in 0.1 M NaOH	0.08 ^b	490	515
T*-fluorescein single strand	0.11 ^b	495	517
T*-fluorescein duplex	0.16 ^b	492	517
sodium 1-pyrenesulfonate	1.0 ^c	346	376
<i>N</i> -(1-pyrenesulfonyl)ethylenediamine	0.70 ^c	351	381
T*-pyrenesulfonate single strand	0.24 ^c	354	384
T*-pyrenesulfonate duplex	0.06 ^c	357	384
1-pyrenebutanoic acid	1.0 ^d	342	376
T*-pyrenebutyrate single strand	0.02 ^d	348	377
T*-pyrenebutyrate duplex	0.002 ^d	352	378

^a All samples in air-saturated T_m buffer solution at 20 °C except as otherwise noted. ^b Using fluorescein in 0.1 M NaOH as a standard; excitation = 410 nm, emission = 450–700 nm. ^c Using pyrenesulfonate in T_m buffer as a standard; excitation = 320 nm, emission = 350–500 nm. ^d As in *b*, except using pyrenebutyrate in T_m buffer as a standard.

two are the stable forms of the free labels present in aqueous solution (in this case the pH 7, T_m buffer is used), since hydrolysis of the *N*-hydroxysuccinimide ester and sulfonyl chloride groups occurs. The fluorescein derivative, 5-((2-aminoethyl)thioureidyl)fluorescein, was also used for comparison. This molecule is formed by the reaction of ethylenediamine with 5-(isothiocyanato)fluorescein, in analogy with the DNA-labeling reaction. The absorption due to fluorescein in the labeled oligomers is similar to that of fluorescein alone. It is interesting to note that there is a slight red shift in both the fluorescein-labeled single strand (Figure 3A) and the thiourea derivative (not shown; see Table II), while in the duplex (Figure 3B) this shift is absent. In the single-strand form, the bases are available for hydrogen bonding and π -stacking interactions with the fluorescein label. The former interaction is also possible in the thiourea derivative via the ethylenediamine moiety. Duplex formation significantly lessens these interactions and restores the spectral appearance of free fluorescein. For the pyrenebutyrate-labeled oligomer, both the single strand (Figure 3D) and duplex (Figure 3E) have label absorption bands qualitatively like those of free pyrenebutyrate (Figure 3F). Thus conversion of pyrenebutanoic acid to a pyrenebutyramide derivative as a result of the labeling reaction apparently does not significantly affect the appearance of the label's spectrum. This is not surprising, since the carboxylic acid functional group is electronically isolated from the pyrene chromophore by three methylene groups. In striking contrast, the absorption spectrum of pyrenesulfonate-labeled DNA is quite different from that of pyrenesulfonate (or from that of a fresh solution of 1-pyrenesulfonyl chloride). This results from formation of the sulfonamide linkage between 1-pyrenesulfonyl chloride and the primary amine on the modified oligomer. This explanation is supported by the similarity between the absorption spectra of the pyrenesulfonate-labeled single strand (Figure 3G) and pyrene with an authentic sulfonamide linkage (Figure 3J). Since the sulfonyl group is directly bonded to the pyrene chromophore, conversion of a sulfonate to a sulfonamide can affect the pyrene chromophore's π -electrons and thus alter its absorption spectrum. This spectral change also provides direct spectroscopic evidence that the labeling reaction gave the expected product. The sulfonamide can result only from the reaction of pyrenesulfonate with a primary amine, and only the C* and T* containing oligomers with their primary amine linker arms gave this product.

The covalent attachment of a DNA octamer, with its numerous functional groups, to a fluorescent label can provide many pathways for nonradiative relaxation of the label's electronic excited states. This effect can be seen by comparison of the emission quantum yields and spectra for the labeled single strands relative to the free labels. Evidence suggesting label intercalation into a DNA duplex can be sought by comparing the emission properties of the labeled duplex to those of the corresponding labeled single strand. Table II summarizes the fluorescence

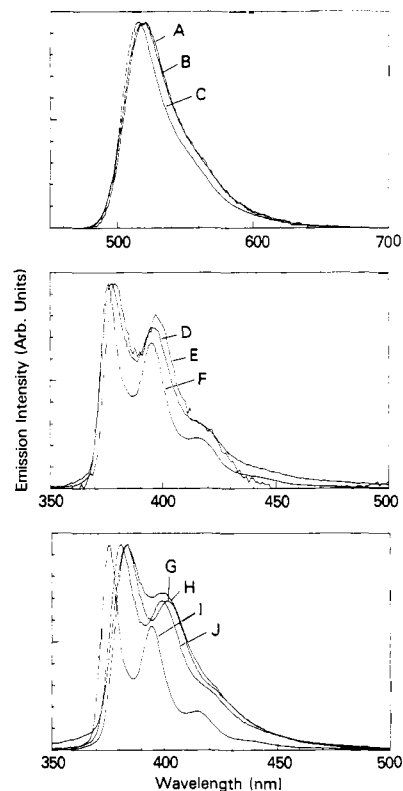


Figure 4. Normalized emission spectra of fluorophore-labeled DNA and free fluorophores: (A) fluorescein-labeled single strand; (B) fluorescein-labeled duplex; (C) fluorescein; (D) pyrenebutyrate-labeled single strand; (E) pyrenebutyrate-labeled duplex; (F) pyrenebutyrate; (G) pyrenesulfonate-labeled single strand; (H) pyrenesulfonate-labeled duplex; (I) pyrenesulfonate; (J) *N*-(1-pyrenesulfonyl)ethylenediamine. Excitation is at 320 nm for pyrene and at 410 nm for fluorescein. All samples are in the pH 7 T_m buffer described in the text, and the spectra are corrected for buffer background emission.

quantum yield data obtained for the labeled oligomers relative to those for the free labels. Figure 4 shows the emission spectra for the fluorophore-labeled oligomers. Excitation spectra (not shown) were also obtained by monitoring the emission at 380 nm for the pyrene and at 525 nm for the fluorescein-labeled duplexes. Both the emission and excitation spectra of the labeled oligomers were qualitatively the same as those of the free labels. However, in all cases, covalent attachment of a fluorescent label to the DNA oligomer led to significant quenching of the label's emission.

In addition to intramolecular association between a label and its attached oligomer, another possible effect leading to emission quenching is that of intermolecular association between a label and another oligomer. As discussed above the sequence chosen is not self-complementary, so there is no oligomer-based driving force for association between labeled single strands; indeed electrostatic repulsion between the negatively charged single strands should disfavor intermolecular association. The only driving force for intermolecular association is that of the hydrophobic label seeking a less hydrophilic environment. However, it is unlikely that in the low concentrations used here (micromolar), this would be favored over intramolecular effects for which the effective concentration is much higher. Unfortunately, emission quantum yields can be measured accurately only at high dilution, so the concentration dependence of the emission quantum yields can be studied only over a narrow concentration range.

There is little difference in emission quantum yield between the fluorescein-labeled octamer as a single strand and as a duplex. Both exhibit significant quenching compared to either fluorescein or the fluorescein thioureidyl derivative. The latter two quantum yields are roughly equal, which indicates that the thiourea linkage itself has no significant effect on fluorescein emission. The quantum yield for the labeled single strand is slightly lower than that for the labeled duplex. This trend is consistent with their

absorption spectra, which showed the absorption band of the duplex more closely resembling that of the free fluorescein label. The emission quantum yield of fluorescein is very sensitive to environment, and apparently interaction with functional groups on DNA leads to this quenching. An example of this sensitivity can be seen by comparison of the quantum yields for the two types of fluorescein as a function of pH. The emission quantum yield of fluorescein is the same in 0.1 M NaOH as in the pH 7 T_m buffer. However, the thioureidyl derivative has a quantum yield roughly equal to fluorescein when at pH 7 but is very strongly quenched (>10 times) in the basic solution. The terminal primary amine can act as a reductive quencher of fluorescein emission in the basic solvent where it is unprotonated but not in the pH 7 solution where it is protonated.

The pyrene-labeled oligomers showed greater differences in emission yields between their single strand and duplex configurations. A 4-fold decrease in quantum yield is seen for the pyrenesulfonate-labeled single strand when compared to pyrenesulfonate, and a 3-fold one is found when compared to *N*-(1-pyrenesulfonyl)ethylenediamine. The latter pyrene derivative shows pH dependent emission quantum yield behavior very similar to that described above for the fluorescein thioureidyl species. In 0.1 M HCl, the quantum yields for pyrenesulfonate and its ethylenediamine derivative are roughly equal. However, in 0.1 M NaOH the quantum yield of pyrenesulfonate remains virtually the same, while that of *N*-(1-pyrenesulfonyl)ethylenediamine is reduced by >100 times. A pH-dependent reductive quenching mechanism similar to that described above for fluorescein is likely here as well. The ethylenediamine derivative of pyrenesulfonate showed greater emission quenching relative to pyrenesulfonate at high pH than did the analogous fluorescein derivative relative to fluorescein ($100\times$ versus $10\times$). This may be due to reductive quenching by the deprotonated sulfonamide nitrogen (pK_a approximately 10) in addition to quenching by the primary amine nitrogen present in both derivatives. As for fluorescein, pyrene's emission yield is thus shown to be sensitive to chemical environment. Comparison of the pyrenesulfonate-labeled single strand to its duplex shows a 4-fold lower quantum yield in the duplex configuration. The pyrenebutyrate-labeled single strand, in contrast, shows approximately 50 times less emission than does its corresponding free label, and its duplex shows about 500 times less emission. In fact, the small emission yield observed for the pyrenebutyrate-labeled duplex may be due to a small amount of labeled single strand DNA. As will be discussed below, at 20 °C roughly 98% of the DNA is in the duplex form leaving the remainder as single strands. The high degree of emission quenching seen in the pyrene-labeled duplexes is consistent with intercalation of pyrene into the base-pair stacking region. However, significant emission quenching is also seen for pyrene-labeled single strands where intercalation is not possible. It is possible that intermolecular association occurs in both these cases. However, as described above for the labeled single strands this is unlikely at the low concentrations used here, although concentration-dependent quantum yields cannot be measured accurately to confirm this.

The above quantum yield results indicate that emission quenching in octameric duplexes is far more efficient for pyrenebutyrate than for pyrenesulfonate. Both steric and electronic reasons can be proposed to rationalize this difference. In the case of the pyrenebutyrate-labeled oligomer, the linker arm contains 11 atoms (from C-5 on the pyrimidine to C-1 on the pyrene), while the pyrenesulfonate linker arm consists of 8 atoms. The longer linker arm with more degrees of freedom should allow a pyrene label to intercalate more effectively, and a sulfonyl group at C-1 on pyrene will sterically hinder intercalation more than a methylene group at the same position. Very importantly, the electron-withdrawing property of a sulfonyl group compared to an electron-donating aliphatic chain may make the pyrenesulfonate label a poorer electron donor than pyrenebutyrate. Electron transfer from the excited state of pyrene to a heterocyclic base in DNA (followed by rapid charge recombination) can provide a very rapid, nonradiative relaxation pathway. This pathway would, therefore, be less favored for pyrenesulfonate compared

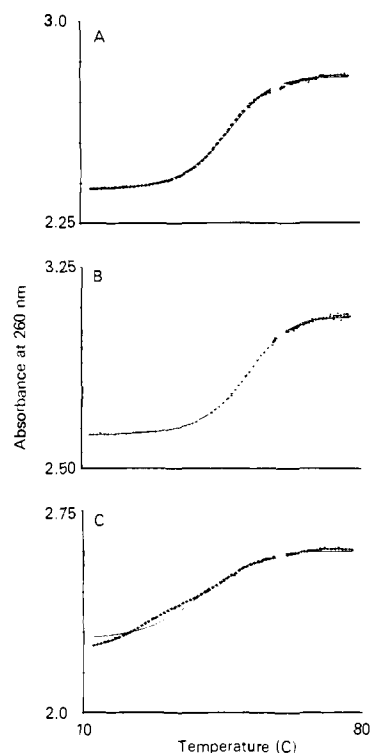


Figure 5. Melting curves of octanucleotide duplexes: (A) unmodified duplex; (B) duplex labeled with pyrenebutyrate at T^* ; (C) duplex labeled with pyrenebutyrate at C^* . The high-temperature to low-temperature experimental curve is shown (plus signs) together with a best nonlinear least-squares fit (solid line) using the "all-or none" model (see text for description). The absorbance was monitored at 260 nm in a 1-cm path length cell, and the temperature was ramped at 10 °C/h.

to pyrenebutyrate. Similar steric and electronic factors are also likely to contribute to differential emission quenching in the pyrene-labeled single strands. In related studies of oligomers with acridine derivatives attached at terminal phosphorus,^{11-13,15} quenching was seen only when intercalation involved a GC base pair. Intercalation between AT pairs actually led to an increase in emission quantum yield. However, in a study of the interaction of benzopyrene derivatives with natural DNA, Geacintov et al.³⁰ found the converse to be true: emission quenching occurred more strongly in the presence of AT base pairs. The octameric sequence studied here contains five GC and three AT pairs. However, there are no adjacent AT pairs and only one adjacent GC pair (at one end of the duplex). Therefore, almost all intercalation sites have both AT and GC base pairs present, and no conclusion can be drawn as to preferential emission quenching by the different types of base pairs.

Thermodynamic Characterization. Melting curves at a series of DNA concentrations were recorded for a number of duplexes. The thermodynamic results are summarized in Table I. None of the oligomers containing a molecular label covalently linked to cytidine (C^*) gave the desired melting curve behavior (see below). This can be seen graphically in Figure 5, which presents the melting curves of the unmodified octamer (Figure 5A) and of the octamers in which pyrenebutyrate was covalently attached to thymidine (Figure 5B) and to cytidine (Figure 5C). The best fit to each of these curves is also indicated. It is apparent that curves 5A and 5B are qualitatively identical, while 5A and 5C are not. Additionally, curves 5A and 5B can be accurately fitted to the "all-or-none" model. Curve 5C in contrast is impossible to fit by using this model, since it shows at least a two-phase hybridization process. Detailed analysis of such melting curve behavior is beyond the scope of this work; however, it is clear that the mechanism of duplex formation was significantly changed by covalent attachment of a label to cytidine. In this study, all of the oligomers with labels attached to cytidine gave curves that show hypochromicity as the temperature is lowered but lack a

single helix-to-coil transition point. This hypochromicity suggests that duplex formation is occurring, but via a mechanism that is different from the expected "all-or-none" model. Two-phase behavior, however, was not always as apparent as in Figure 5C. In contrast, the modified oligomer that contained only a linker arm attached to cytidine showed normal T_m behavior. The linker arm itself, 1,3-propanediamine, is sterically undemanding and terminates in a water-soluble primary amine. Apparently it is sufficiently noninteracting with the DNA strands that base pairing is not seriously disturbed. The resulting duplex was less stable than the corresponding unmodified duplex but no less stable than the duplex containing a modified thymidine. Presumably, particular octamers with noninteracting labels attached to cytidine will show normal melting curve behavior.³³ However, this work demonstrates that T* labeling will more generally produce duplexes with normal melting curve behavior than will C* labeling.

Given that it was not possible to fit the melting curves for octamers with labeled cytidines, no meaningful thermodynamic parameters can be obtained for these systems. It is, however, a qualitative result that covalent attachment of a label to a site directly involved in base pairing can significantly perturb DNA hybridization. This was true both for a water-insoluble label, such as pyrene, and for a water-soluble label, such as fluorescein. This hybridization perturbation for oligomers labeled by means of a modified cytidine suggests that a similar problem may occur for attachments to 4-thiouridine. In this case,⁵ the label is attached to a sulfur which is involved in base pairing.

In the thymidine-modified octamers, it was possible to measure the thermodynamic parameters for duplex formation. The melting curves were well fitted to yield accurate T_m values, and a linear dependence of $1/T_m$ on \ln (octamer concentration) was found. This allowed determination of ΔH° and ΔS° for duplex formation (see Table I). Given the good fits to all sections of the melting curve, it is also possible to calculate the fraction of DNA in the duplex form at a given temperature. For example, for the unmodified oligomer with a total absorbance of 1, approximately 98% of the strands are hybridized at 20 °C. Similar values are true for the other labeled octamers. Therefore, the absorption and fluorescence spectra measured at 20 °C (see Figures 3 and 4) were due almost entirely to duplex DNA when the complementary strands were present.

The effect of attached labels on duplex formation can be assessed in several ways. Comparison can be made between a labeled duplex and (1) the corresponding duplex containing only the linker arm, (2) the corresponding unmodified duplex, or (3) the corresponding heptameric duplex, in which the modifiable base and its partner are absent. Comparison with the corresponding unmodified duplex is important, since the linker arm is an unavoidable feature in the covalent attachment of labels to oligonucleotides. However, comparison with the duplex containing the linker arm alone is necessary to assess the relative effects of different labels. Comparison to the heptameric duplex is useful in determining whether the base modification or label attachment has the effect of negating the entire stabilizing contribution of that base pair.

The effect of the linker arm alone can be considered first. At pH 7, the primary amine linker arm is protonated and could thus help counteract the electrostatic barrier to duplex formation by the negatively charged oligomers. Nevertheless, a net destabilization of duplex formation (by roughly 1 kcal/mol in ΔG°) is seen for both C* and T* octamers compared to the unmodified octamer. In fact this result may simply indicate that the single strand forms are more stable due to internal electrostatic effects, while the duplex stability is not significantly changed. It is interesting to note that the T* duplex has the same ΔG° (-9.9 kcal/mol) as the duplex formed between 5'-GCACCAG-3' and 5'-CTGGTGC-3', the heptamer duplex lacking the AT* pair. This

shows that modification of the internal thymidine with a primary amine linker arm has the same result on relative duplex stability as removal of that base. It is important to point out here that nearest-neighbor as well as base-pairing interactions are important in determining duplex stability.³⁴ Therefore, the loss of an AT pair may be somewhat offset by the formation of CC/GG nearest neighbors. Breslauer et al.³⁴ report that a CC interaction is nearly twice as stable as those of CT or TC. To analyze the effect of thymidine modification more fully, it would be necessary to compare sequences containing T(T*)T versus TT. The duplex containing only the C* modification gave the same ΔG° as the one with T* only. However, the corresponding heptameric duplex, formed by 5'-GCATCAG-3' and 5'-CTGATGC-3', was less stable by 1.4 kcal/mol. In this case, removal of a GC base pair has a dramatic effect on duplex stability, because the nearest neighbors change from ACT/TGA to AT/TA, and nearest-neighbor compensation effects are not present as was true for the T* modification.

Label Characteristics. A biotin label is of interest for avidin-based colorimetric detection assays.³⁵ Labeling with biotin does not adversely affect qualitative duplex formation, but it does destabilize the duplex by 1.5 kcal/mol relative to the unmodified duplex and by 0.6 kcal/mol relative to T*. Biotin has no ability to intercalate, is uncharged, and is smaller than pyrene or fluorescein. Furthermore, this biotin derivative has a hexanoate spacer between the biotin moiety and the linker arm. This "long-chain" biotin is frequently chosen to minimize steric interference when binding to avidin.³⁶ Thus biotin can be positioned the most distant from the T* attachment of all the labels studied here. It therefore represents an ideal label in terms of minimizing possible interferences to duplex formation (see also ref 33). The duplex destabilization seen here is probably the consequence of unavoidable steric interactions between the duplex and an attached label. It is unlikely that biotin helped stabilize the free strands, so this destabilization may be a good estimate of the minimum achievable destabilization by a label attached to T*.

Attachment of fluorescein to a modified octamer gave melting curves with qualitatively the same appearance as those of the unmodified duplex, but duplex formation in this case had a significantly less negative ΔH° value of -41 kcal/mol than in the cases of the above described duplexes (see Table I). ΔG° for this duplex is about the same as that for the biotin-labeled duplex. Intercalation of fluorescein would be expected to lead to stabilization of the duplex and perhaps emission quenching as well. Such effects have been seen in oligomers with fluorescent labels attached at phosphorus.^{10,15} Neither phenomenon was seen here with fluorescein. The increase in ΔH° seen with fluorescein was large whether compared to the unmodified or linker-arm-only duplex. Two factors may cause this effect. First, interactions between the attached fluorescein and the single strand octamer may be stronger than in the above two cases. Fluorescein does have functional groups that can interact with DNA. Second, fluorescein may interfere with duplex formation either sterically or electrostatically. Fluorescein at pH 7 has a double negative charge with increases the net negative charge of the labeled strand at this pH. This may increase the electrostatic barrier that must be overcome to form the duplex. A more detailed study involving T_m determinations at different salt concentrations for a series of labeled and unmodified oligomers may be able to clarify this point.

In contrast to the above results for fluorescein, the octamer labeled with pyrenebutyrate showed significant duplex stabilization: $\Delta H^\circ = -54$ kcal/mol, and $\Delta G^\circ = -11.4$ kcal/mol. In fact these thermodynamic values are nearly the same as those for the unmodified octamer. The combination of duplex stabilization and quenching of pyrene emission suggests that the pyrenebutyrate label is binding to the helix and perhaps intercalating into it. The octamer labeled with pyrenesulfonate represents an intermediate

(33) A modified cytidine (C* type) has been synthesized by using 1,6-diaminohexane rather than 1,3-diaminopropane. Duplexes were prepared containing this aminohexyl-modified cytidine alone and with biotin-LC attached; both displayed normal melting behavior that could be fit by the "all-or-none" model, respectively, $\Delta G^\circ = -9.2$ and -8.1 kcal/mol.

(34) Breslauer, K. J.; Frank, R.; Blocker, H.; Marky, L. A. *Proc. Natl. Acad. Sci. U.S.A.* **1986**, *83*, 3746.

(35) Green, N. M. *Methods Enzymol.* **1970**, *18A*, 418.

(36) Leary, J. J.; Brigati, D. J.; Ward, D. C. *Proc. Natl. Acad. Sci. U.S.A.* **1983**, *80*, 4045.

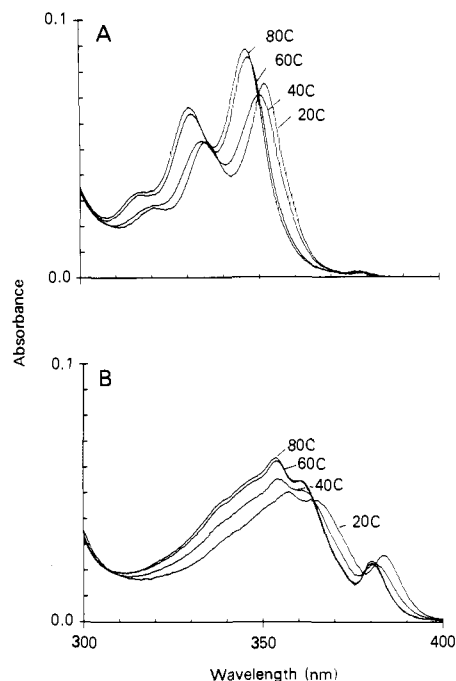


Figure 6. Variable-temperature UV-visible absorption spectra of pyrene-labeled duplexes: (A) pyrenebutyrate; (B) pyrenesulfonate.

case between pyrenebutyrate and fluorescein: $\Delta G^\circ = -10.0$ kcal/mol. For the steric and electronic reasons given above, pyrenesulfonate is expected to be a poorer intercalator than pyrenebutyrate. ΔG° for the pyrenesulfonate-labeled duplex is the same as that for the linker-arm-only duplex; however this was achieved by compensating changes in the values of ΔH° and ΔS° .

The duplex stabilization seen here for pyrenebutyrate is considerably less than the ΔG° decrease of 5.5 kcal/mol seen for an acridine derivative covalently attached via a hexamethylene linker arm to the 3'-phosphate of dodecathymidine hybridized to poly(dA).¹⁵ However, it is difficult to compare the study of Helene et al.¹⁵ to this work, since there are differences in base sequence, label, linker arm, salt concentration, and mode of label attachment. However, the greater stabilization seen for the phosphate-labeled system may be due in part to steric effects. Covalent attachment as a terminal phosphate should not interfere with helix stability nearly as much as at an internal base.

Further evidence for interaction between the pyrene labels and their duplexes can be seen in near-UV absorption spectra as a function of temperature. This is shown in Figure 6 for both pyrenebutyrate (Figure 6A) and pyrenesulfonate (Figure 6B) over the 20–80 °C temperature range. At 20 °C the oligomers are predominantly hybridized, while at 80 °C they are entirely in the single-strand conformation. A red shift of 7 nm for pyrenebutyrate and 3 nm for pyrenesulfonate is seen at 20 °C relative to the absorption positions at 80 °C. Absorption strength in this spectral region generally decreases as the temperature is lowered. For comparison, the absorption spectra of single strands of the two pyrene-labeled oligomers were also measured over this temperature range (not shown). The spectrum of the pyrenebutyrate-labeled single strand showed a light (<2 nm) red shift, while that of pyrenesulfonate showed no shift. Additionally, no significant changes in absorption strength were seen for either single strand. These spectral results indicate that both types of pyrene labels interact much more strongly with a duplex as opposed to a single strand. However, the slight temperature dependence of the absorption of the pyrenebutyrate-labeled single strand is probably significant, since considerable emission quenching (~50 times) was seen for this sample (see Table II). Thus it appears that this label slightly stabilized the single strand as well as strongly stabilizing the duplex form.

Figure 6 shows that a substantial change occurs at 345 nm for both pyrene labels. Consequently, melting curves were obtained

Table III. Comparison of Calculated and Experimental Thermodynamic Parameters for Duplex Formation

sequence	$\Delta H^\circ_{\text{calc}}$	$\Delta H^\circ_{\text{expt}}$	$\Delta G^\circ_{\text{calc}}$	$\Delta G^\circ_{\text{expt}}$
CGTCGACG	-60	-64 (-64 ^b)	-11.2	-12.0 (-11.9 ^b)
GCACTCAG	-50	-56	-8.0	-10.9
GCATCAG	-45	-42	-6.6	-8.5
GCACCAG	-48	-50	-7.9	-9.9

^a All duplexes in 1 M NaCl at pH 7. All parameters in kcal/mol.
^b Reference 34.

by monitoring the absorbance at this wavelength also. The resulting curves for both pyrene labels have the same qualitative appearance as those obtained at 260 nm. In addition, the T_m values obtained from the curves at 345 nm are equal to those measured at 260 nm. Because the pyrene absorption at 345 nm is less intense than that of DNA at 260 nm, it was not possible to span the same concentration range at both wavelengths. Nevertheless, the thermodynamic results at 345 nm are consistent with those based on measurements at 260 nm. Similar melting curve behavior at 345 nm was seen for hexathymidine with pyrenebutyrate attached to an internal phosphorus hybridized to poly(A).¹⁰ Hypochromism arising from label/duplex association was also seen in the studies of oligomers with acridine labels attached at phosphorus.^{11–13,15} However, another experimental technique such as NMR is required to assess fully the extent of intercalation for the two pyrene labels in our system.

Theoretical versus Experimental Thermodynamics. A final area worth comment concerns the thermodynamic results obtained for the unmodified oligomers. A large number of thermodynamic studies have been performed on unmodified oligonucleotides for both DNA and RNA with normal sequences,^{34,37} with base mismatches,^{38,39} and with terminal unpaired bases.^{25,40} Due to this body of work, the experimentally obtained thermodynamic parameters for the unmodified octamer and the two heptamers studied here can be compared to the theoretical values calculated by using the method of Breslauer et al.³⁴ Their method sums experimentally determined nearest-neighbor interactions to give predicted thermodynamic parameters for an entire oligonucleotide.

Table III summarizes the experimentally determined and predicted thermodynamic parameters for the three unmodified duplexes studied here. Additionally, a self-complementary octanucleotide that had been previously studied by Breslauer et al.³⁴ was reexamined in this work. This octamer was chosen for its length and for the similarity of its sequence (5'-CGTCGACG-3') to that of the octamer used in this work (5'-GCACTCAG-3'). It was prepared and purified with the same procedures as used for the other oligomers studied here. Finally, the agreement between the experimental thermodynamic parameters determined in this study for this self-complementary octamer and the values previously reported (see Table III)³⁴ was exact.

The agreement between the experimental and predicted ΔH° values is acceptable and is comparable to that for many of the previously reported duplexes.³⁴ However, as good agreement is not found for the ΔG° values. This discrepancy may be due to the choice of sequences. Many of Breslauer's sequences are self-complementary. Furthermore, many of the sequences contain predominantly internal AT base pairs. The sequences described in this work are not self-complementary and have more alternating AT and GC base pairs. Since the ΔH° values are in reasonable agreement with theory, the problem with ΔG° may arise from errors in ΔS° , which is more difficult to measure. The entropic contribution plays a role in self-complementary versus non-self-complementary sequences and in nearest-neighbor interactions. Perhaps thermodynamic parameters for a wider range of sequences

(37) Cantor, C. R.; Schimmel, P. R. *Biophysical Chemistry, Part I. The Conformation of Biological Macromolecules*; W. H. Freeman: San Francisco, 1980; Chapter 6.

(38) Aboul-ela, F.; Koh, D.; Tinoco, I., Jr.; Martin, F. H. *Nucleic Acids Res.* **1985**, *13*, 4811.

(39) Arnold, F. H.; Wolk, S.; Cruz, P.; Tinoco, I., Jr. *Biochemistry* **1987**, *26*, 4068.

(40) Petersheim, M.; Turner, D. H. *Biochemistry* **1983**, *22*, 256.

need to be measured and incorporated into Breslauer's evaluation of nearest-neighbor interactions.³⁴

Summary and Conclusions

Using chemically modified bases and standard automated oligonucleotide synthesis procedures, it is possible to prepare DNA oligomers containing internal primary amine groups that can be selectively linked to a variety of molecular labels. Successful duplex formation can occur at room temperature with oligonucleotides as short as octamers even with an internally attached label. However, the covalent attachment to an internal heterocyclic base at a position that is involved in base pairing can perturb duplex formation. The electronic absorption and emission features of the fluorescent labels used here were maintained in the labeled oligomers, but significant emission quenching occurred for both the single strand and duplex systems in some cases. This was especially true for the oligomers labeled with pyrenebutyrate: fluorescence from this label was nearly completely quenched in the duplex. This fluorophore was attached by a long and flexible linker arm to the base and thus could easily associate with or intercalate between base pairs, allowing rapid radiationless decay, quite possibly due to excited-state electron transfer to these bases. In cases where the label should remain spectroscopically observable in both single-strand and duplex forms of DNA, the covalent attachment of the label to an internal base should employ a more rigid linker arm than that used here. Sometimes the destabilizing effect of attaching a linker arm to a duplex can be overcome by label/duplex association. However, in systems that prevent such association the internally labeled duplex will probably be less stable than the corresponding unmodified duplex. This work demonstrates both the feasibility of covalent attachment of internal labels

(or reporter groups) to synthetic DNA oligomers and some of the consequences of doing so. In general, attachment of an internal label is less likely to perturb duplex formation if the position of attachment is not involved in base pairing, e.g., desirable attachment sites are position 5 on the pyrimidine ring and position 8 on the purine ring. Additionally, relatively inflexible linker arms are likely to reduce label/duplex association. The latter can be constructed, for example, by use of piperazine rather than ethylenediamine in the synthesis of a modified thymidine. Other synthetic alternatives are also possible. Such inflexible linker arms could still permit intermolecular association between labels and separate duplexes. However this type of association should be infrequent at low concentrations and for hydrophilic labels.

Acknowledgment. We gratefully acknowledge the technical assistance of Raymond J. Carroll, Daniel L. Stockwell, and Lucy M. Stols (all of Amoco Technology Co.). We thank Professor Robert L. Letsinger for many helpful discussions and Doris Hung for obtaining the mass spectral data (both of Northwestern University). We thank a reviewer for helpful comments.

Registry No. H₂N(CH₂)₃NH₂, 109-76-2; **2**, 109082-26-0; **3**, 109082-27-1; **4**, 109082-28-2; **5**, 121351-62-0; **6**, 65505-76-2; **7**, 96203-39-3; **7** (5'-DMT derivative), 96203-40-6; **8**, 96203-41-7; **9**, 121329-87-1; **10**, 121329-88-2; GCACTCAG, 121329-89-3; GCA(C*)TCAG, 121329-90-6; GCAC(T*)CAG, 121351-63-1; GCAC(T*-biotin-LC)CAG, 121329-91-7; GCAC(T*-fluorescein)CAG, 121329-92-8; GCAC(T*-pyrenebutyrate)CAG, 121329-93-9; GCAC(T*-pyrenesulfonate)CAG, 121351-64-2; GCATCAG, 121351-65-3; GCACCAG, 121351-66-4; H₂N(CH₂)₃NH₂, 109-76-2; H₂C=CHCOOMe, 96-33-3; H₂NCH₂-H₂NH₂, 107-15-3; 2'-deoxyuridine-5-(propenoic acid methyl ester), 96244-97-2; biotin, 58-85-5; fluorescein, 2321-07-5; pyrene, 129-00-0.

Multiply Charged Isoelectronic Analogues of C₃H₃⁺: Cyclic or Open Chain?

Ming Wah Wong and Leo Radom*

Contribution from the Research School of Chemistry, Australian National University, Canberra, A.C.T. 2601, Australia. Received March 22, 1989

Abstract: The structures and stabilities of the isoelectronic multiply charged analogues of cyclic (cyclopropenyl cation) and open-chain (propargyl) isomers of C₃H₃⁺, namely C₂H₃N²⁺, CH₃N₂³⁺, C₂H₃O³⁺, H₃N₃⁴⁺, CH₃NO⁴⁺, and C₂H₃F⁴⁺, have been investigated by ab initio molecular orbital theory. Fourth-order Møller-Plesset perturbation theory (MP4) with a triple- ζ valence plus d,p-polarization basis set (6-311G**) was employed on MP2/6-31G*-optimized geometries. In contrast to C₃H₃⁺, for which the preferred isomer is the cyclopropenyl cation, the multiply charged analogues are found to prefer open-chain structures. The global minimum on the C₂H₃N²⁺ potential energy surface is the open-chain CH₂NCH²⁺ dication (C_{2v}). Although the cyclic isomer, $\overline{\text{CHNHCH}}^{2+}$, represents a stable form of C₂H₃N²⁺, it lies 35 kJ mol⁻¹ higher in energy than the open structure. The CH₂NCH²⁺ ion is calculated to be thermodynamically stable with respect to proton losses and C-N bond cleavages and, hence, should be readily observable. The cyclic structure is also predicted to be a potentially observable C₂H₃N²⁺ isomer. For the CH₃N₂³⁺ trication, the lowest energy species corresponds to the open-chain NH₂NCH³⁺ (C_{2v}) structure. The cyclic structure, $\overline{\text{NHCHNH}}^{3+}$, lies close in energy, 39 kJ mol⁻¹ above NH₂NCH³⁺. These triply charged ions are characterized by highly exothermic fragmentation reactions. However, such dissociation reactions are inhibited by significant barriers. Thus, NH₂NCH³⁺ and $\overline{\text{NHCHNH}}^{3+}$ are predicted to be experimentally accessible in the gas phase. As in the case of C₂H₃N²⁺ and CH₃N₂³⁺, the C₂H₃O³⁺ system also favors an open-chain structure, CH₂COH³⁺ (C_{2v}). The cyclic structure, $\overline{\text{CHOHCH}}^{3+}$, in this case represents a high-energy isomer. However, both C₂H₃O³⁺ isomers are calculated to have very small barriers (less than 2 kJ mol⁻¹) associated with deprotonation reactions and, therefore, are unlikely to be observable in the gas phase. No stable equilibrium structures were found for the quadruply charged analogues of C₃H₃⁺, namely H₃N₃⁴⁺, CH₃NO⁴⁺, and C₂H₃F⁴⁺. The results of high-level calculations on the cyclopropenyl and propargyl cations are in very good agreement with experimental data.

The cyclopropenyl cation (**1**) is the simplest possible aromatic system with two delocalized π -electrons. This cyclic carbocation

is a commonly observed species in gas-phase mass spectrometric experiments.¹ It is stable in the form of salts and also in polar